Biochemical and structural characterization of the complex agarolytic enzyme system from the marine bacterium *Zobellia galactanivorans*

Jan-Hendrik Hehemann[1,2,3], Gaëlle Correc[1,2], François Thomas[1,2], Thomas Bernard[4], Tristan Barbeyron[1,2], Murielle Jam[1,2], William Helbert[1,2‡], Gurvan Michel[1,2*] and Mirjam Czjzek[1,2*]

## Supplemental Material

Table S1. Design of oligonucleotide primers for six selected target genes from *Z. galactanivorans*

| **Abbrevation** | **Cloning strategy** | **Primer Forward** | **Primer Reverse** |
|---|---|---|---|
| PorAcat | BamH1/EcoRI | gggggggATCCCAATTACCATCTCCTACAAACGGG | CCCCCCgAATTCTTAGTCAACCAATTTATACACCCGTACC |
| PorB | BamH1/EcoRI | gggggggATCCCAAGAAGCTCCACATTTTAAGCCTG | CCCCCCgAATTCTTAATTCTTTGAATCAACCAATTGCCATG |
| PorC | BamH1/EcoRI | gggggggATCCTGTAGCAATTCGGGGGATAATGGT | CCCCCCgAATTCTTACAAATCTTCAAGTTGCCATACCCTA |
| PorDcat | BamH1/EcoRI | gggggggATCCCAAGAGCCCCCTAAAACCTATAGT | CCCCCCgAATTCTTAGTCGTTTACATCGACCAATCGGTA |
| PorE | BamH1/EcoRI | gggggggATCCCAGACGCCGCCGCCGCCGG | CCCCCCgAATTCTTATTGATCTACAGGAAGCAAGGTATAC |
| AgaDcat | BglII/MfeI | gggggAgATCTCAATACGATTGGGACAACGTGCC | CCCCCCCAATTgTTAGTTCACAGGTTTGTAAACCCGGAT |

Table S2: Homology matrix displaying sequence identity and similarity between all agarolytic GH16 modules of *Z. galactanivorans*. The values for the percentage of identity are coloured in red and the percentage of similarity in yellow.

| | 1 | 2 | 3 | 4 | 5 | 6 | 7 | 8 | 9 | 10 |
|---|---|---|---|---|---|---|---|---|---|---|
| 1. Zg4203_AgaA | | 35.6 | 19.6 | 32.1 | 25.2 | 19.8 | 27.6 | 22.8 | 20.4 | 24.2 |
| 2. Zg3573_AgaB | 54.2 | | 25.5 | 35.5 | 22.0 | 23.1 | 21.7 | 20.0 | 21.0 | 18.4 |
| 3. Zg4267_AgaC | 37.9 | 46.1 | | 20.6 | 27.5 | 22.6 | 23.9 | 22.8 | 21.9 | 17.9 |
| 4. Zg4243_AgaD | 47.0 | 56.3 | 38.0 | | 21.8 | 20.2 | 21.5 | 17.9 | 18.0 | 21.2 |
| 5. Zg2600_PorA | 43.2 | 38.7 | 44.7 | 36.1 | | 31.8 | 32.7 | 26.9 | 25.1 | 23.3 |
| 6. Zg3628_PorD | 37.6 | 39.6 | 40.2 | 35.5 | 46.2 | | 38.2 | 33.1 | 27.1 | 20.8 |
| 7. Zg3640_PorE | 43.5 | 36.9 | 38.6 | 34.6 | 52.1 | 52.1 | | 36.2 | 25.9 | 23.7 |
| 8. Zg1017_PorB | 42.5 | 37.2 | 39.5 | 34.4 | 48.5 | 50.7 | 50.0 | | 30.0 | 21.0 |
| 9. Zg3376_PorC | 34.4 | 43.9 | 40.9 | 36.1 | 39.8 | 43.0 | 39.8 | 44.5 | | 19.4 |
| 10. Zg236_CgkA | 40.7 | 36.9 | 40.8 | 34.6 | 40.0 | 41.7 | 39.6 | 43.2 | 36.2 | |

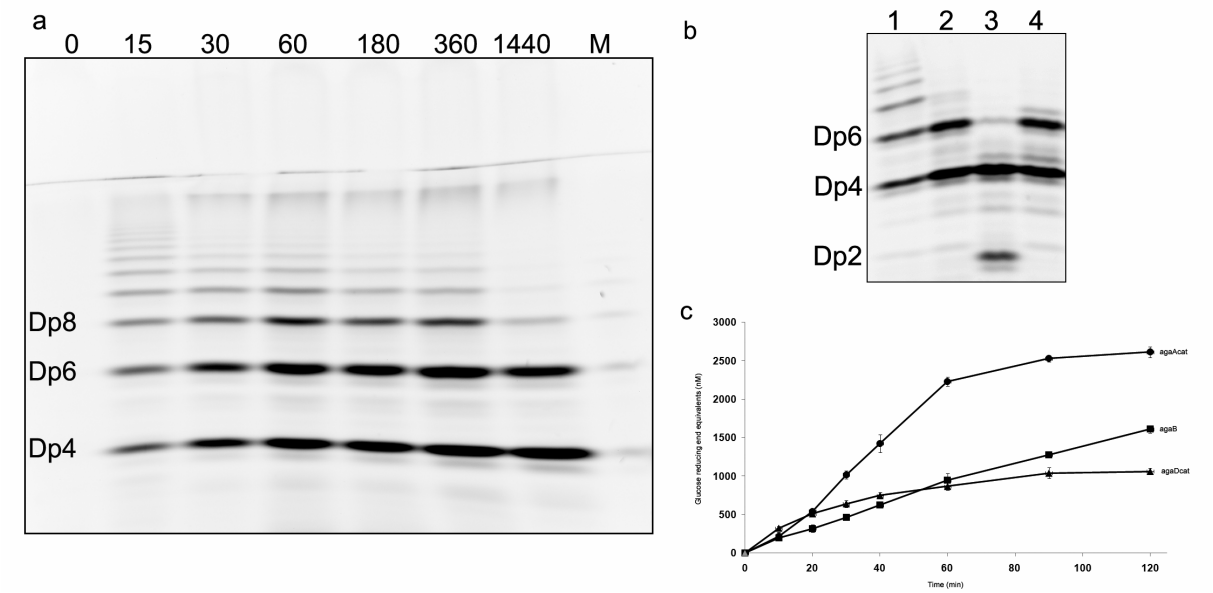


Figure S1. Reaction products of AgaDcat revealed by C-PAGE. a) Gel showing the degradation pattern of AgaDcat incubated with agarose polysaccharide. b) Degradation pattern of DP6 incubated with AgaAcat (lane 2), AgaB (lane 3) and AgaDcat (lane 4). c) Kinetics of agarose degradation by pure agaAcat, AgaDcat and AgaB. AgaD is less efficient on agarose than AgaA and AgaB. A solution with 0.125% agarose (40°C) was incubated with the three enzymes, and aliquots taken at different time-points were analysed by the reducing sugar assay under identical conditions.

**AgaDcat is an endo β-agarase cleaving β-1,4 linkages in agarose**

Description of Figure S1: Due to the low thermostability of AgaDcat, the enzyme was incubated with agarose gel at 30ºC and aliquots were taken for analysis by fluorophore labeled carbohydrate polyacrylamide-gel-electrophoresis (PACE). The produced oligosaccharides were labeled with ANTS and appeared as discrete fluorescent bands. This analysis shows that random sized oligosaccharides are produced by AgaDcat at the onset of the reaction (Figure S1a, lanes 15, 30, 60 min). These oligosaccharides are subsequently degraded to obtain neogarohexose (DP6) and neoagarotetraose (DP4) as final reaction products (Figure S1a, lane 1440 min). Prolonged incubation of DP6 or DP4 agaro-oligosaccharides with high concentrations of AgaDcat did not liberate smaller units (Figure S1b), indicating that these oligosaccharides are the final reaction products of AgaDcat. This is in contrast to AgaB, which was shown to release DP2 and DP4 by degradation of DP6 (Figure S1b and **(18)**), and to a minor extent AgaAcat, which only releases very small amounts of DP2 from DP6 **(18)**.

**Subsite specificity mapping of AgaB, PorA and PorB through the degradation of characterized (hybrid) oligosaccharides**

Since ANTS adds three negative charges per reducing end, any anionic and neutral oligosaccharides modified by this compound migrate to the anode and will be visible on the gel. This does not allow distinction between charged and uncharged oligosaccharides. Thus we used the neutral AMAC to separate anionic from neutral oligosaccharides. Neutral oligosaccharides that do not migrate to the anode are "subtracted" and thereby image complexity is reduced; only hybrid and charged oligosaccharides are visualized. With this technique subtle differences in substrate specificity can be identified for β-agarases and β-porphyranases acting on the heterogeneous natural agars. Here the reaction products of the three β-agarases were compared to those produced by PorA (Figure S2b,c). Both AgaAcat and AgaB produce a number of discrete bands, of which the lowest molecular weight product, present in a double band, had the same velocity as hybrid hexasaccharides with various neoporphyranobiose / neoagarobiose moieties (L6S-G-LA-G-LA-G / L6S-G-L6S-G-LA-G), produced by PorA. Additional bands of lower migration velocity can be identified, but which are present in much lower quantity and here not further characterized. The degradation pattern of AgaDcat is clearly different to the other β-agarases. In particular, no bands of low molecular weight oligosaccharides, produced by AgaAcat or AgaB, are visible after degradation with AgaDcat, even when adding extensive amounts of enzyme. In contrast AgaDcat produces a smear of bands, which migrate with lower velocity and may be interpreted to be hybrid oligosaccharides of much higher molecular weight.

Using AgaB and PorA respectively, we were able to produce and purify a series of neoporphyrano-oligosaccharides, as well as three defined hybrid hexasaccharides with different neoporphyranobiose / neoagarobiose structures (Figure S2a). For the tetra- and one hexa-saccharide a partial separation into a methylated as well as an un-methylated fraction was also obtained. We further investigated the degradation of these oligosaccharides by PorAcat and PorB. Both enzymes degraded the neoporphyranotetraose only in the un-methylated form, showing that the shortest substrate accepted is the tetrasaccharide, but also that both enzymes do not tolerate a methylation of the galactose in the -1 binding subsite (Figure S3). Interestingly PorAcat did not degrade any of the hybrid-hexasaccharides, indicating that this enzyme strictly requires the presence of two consecutive neoporphyranobiose units (L6S-G-L6S-G) for hydrolysis. In contrast, PorB was able to degrade the hybrid hexasaccharide L6S-G-LA-G-L6S-G (Figure S3b), as well as its methylated variant (L6S-G(Met)-LA-G-L6S-G). Since PorB does not accept methylation of the tetrasaccharide at the -1 subsite, we can conclude that the cleavage point of the methylated hexasaccharide is such that the LA unit is bound to the -2 binding subsite.

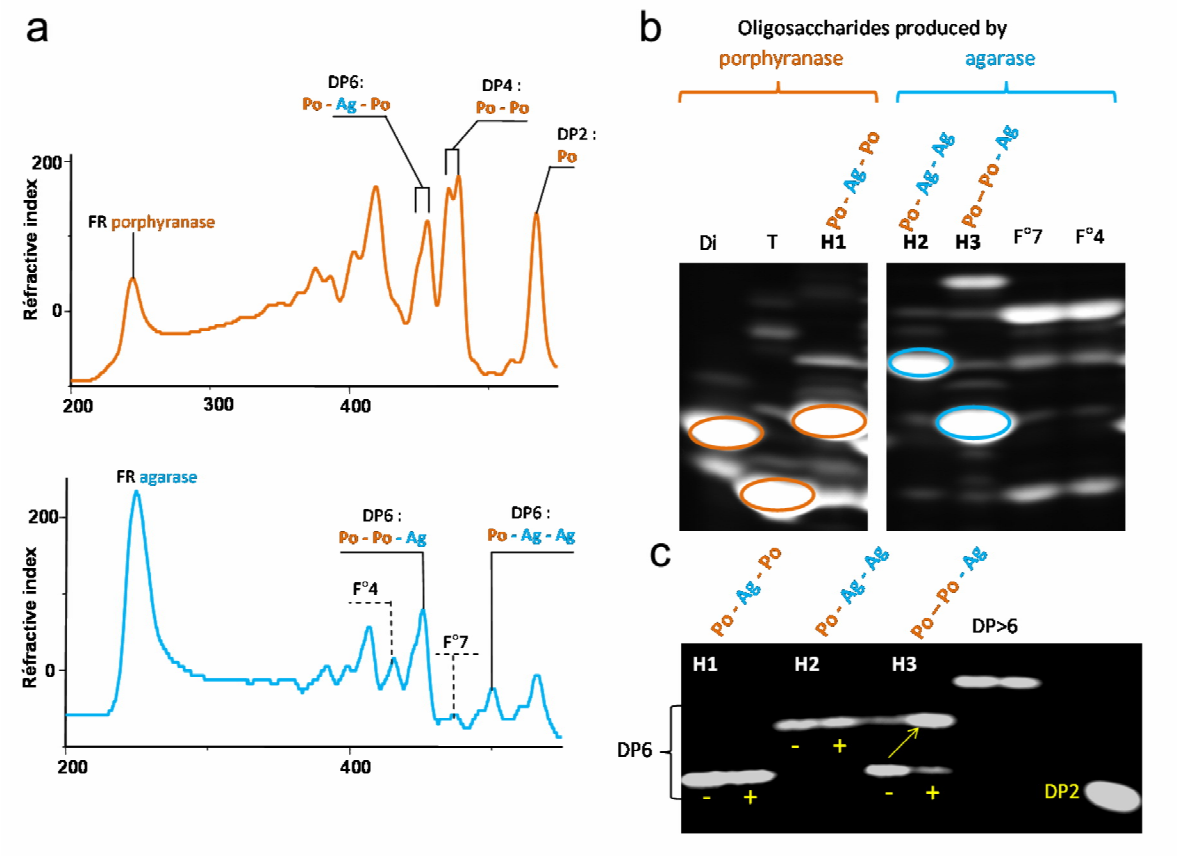


Figure S2a) HPAEC chromatograms of hot-water extracted porphyran degraded by PorA (upper panel) and AgaA (lower panel). b) AMAC PACE of degradation products by AgaB and PorA c) AMAC PACE of degradation products of these characterized hybrid hexasaccharides by PorB.

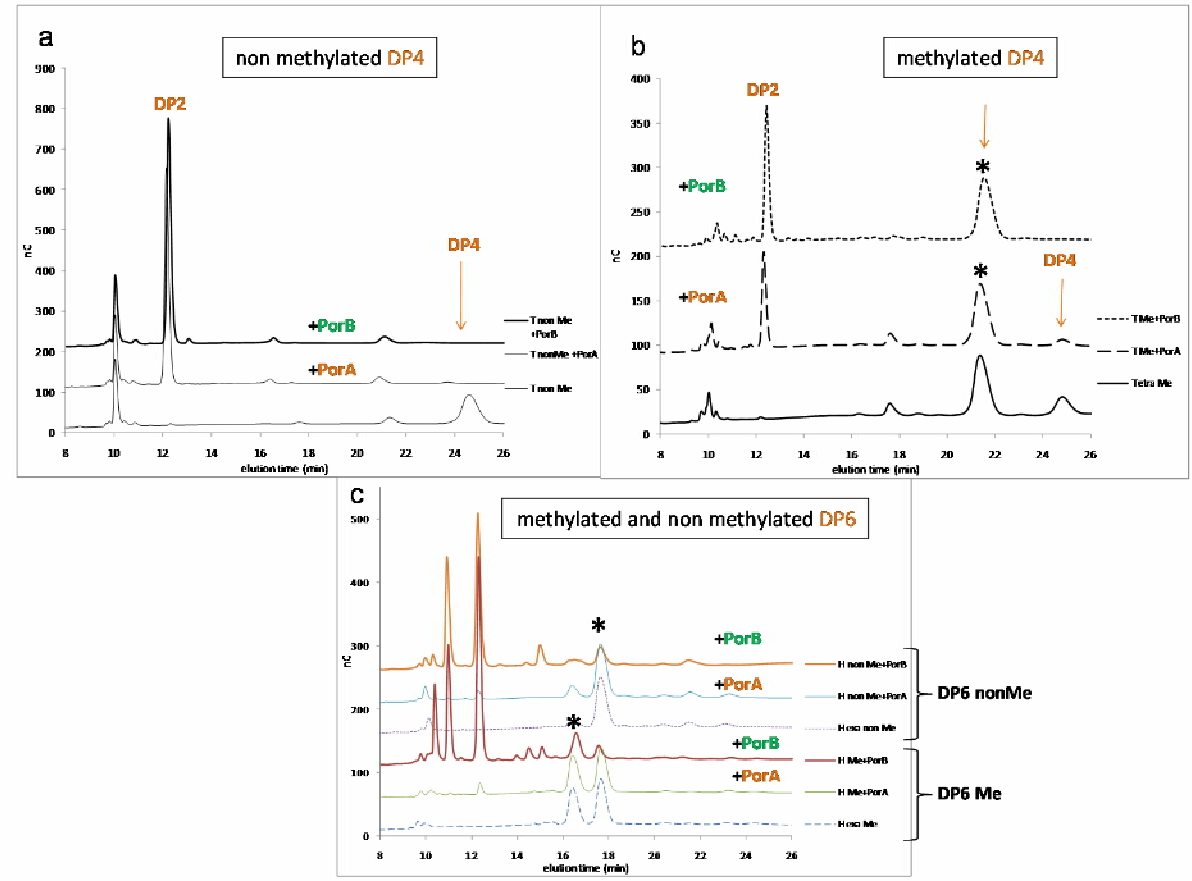


Figure S3. HPAEC chromatograms of degradation by PorA and PorB of a) non methylated, b)methylated porphyrotetraose and c) methylated and non methylated porphyrohexaose.

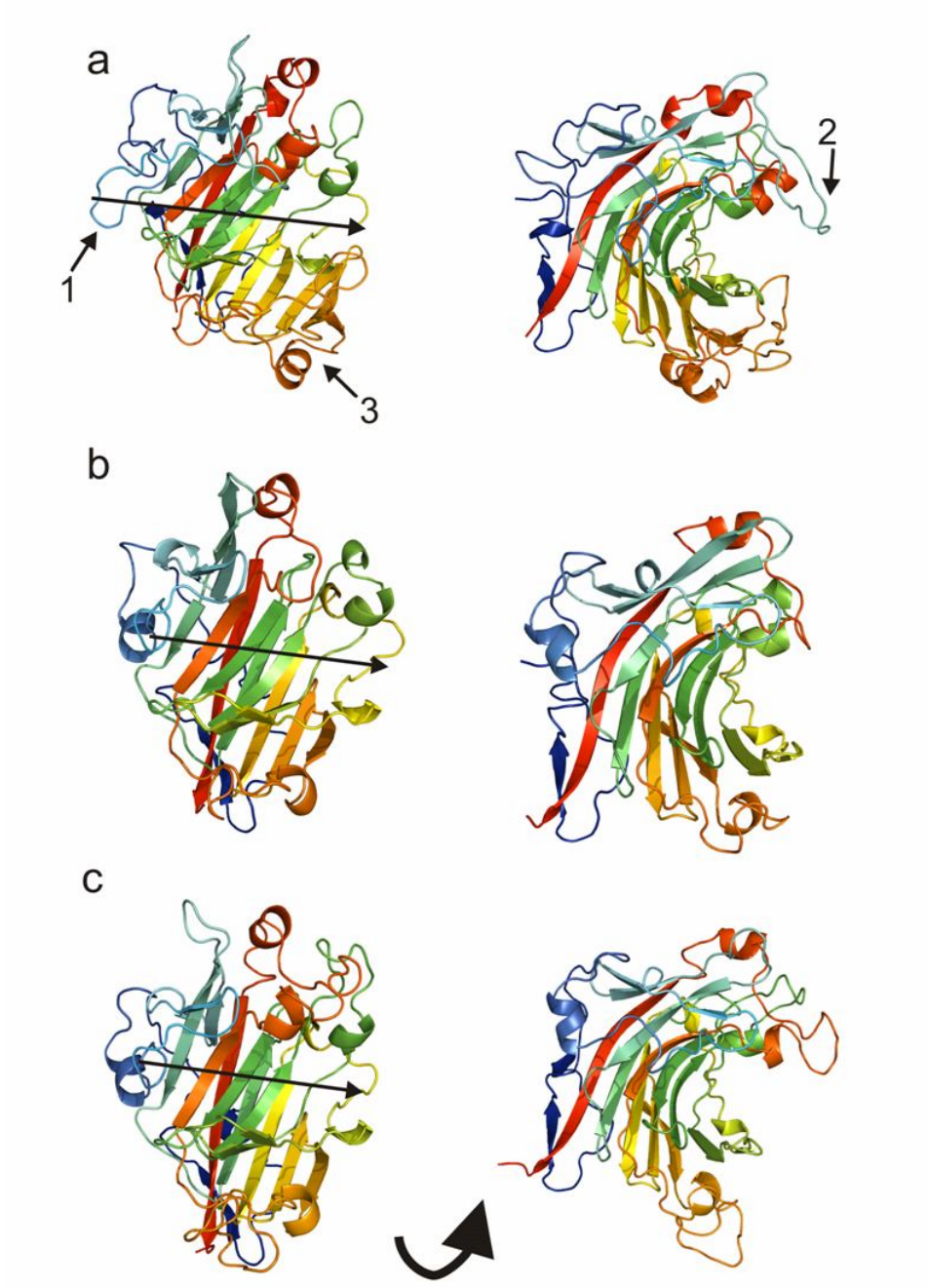


Figure S4. Crystal structure of the β-agarase AgaDcat, as compared to that of AgaAcat and AgaB from *Z. galactanivorans*. The cartoon plots are coloured continuously from the N-terminus in blue to the C-terminus in red. (a) Front view of the substrate binding cleft of AgaDcat and turned by 90°. (b) Front view of the substrate binding cleft ofAgaAcat and turned by 90°. (c) Front view of the substrate binding cleft of AgaB

and turned by 90°. The long arrow indicates binding of substrate in the binding cleft with its tip directing towards the reducing end of the substrate chain. The small arrows shown in (a) point towards the three major loop insertions present in AgaDcat.

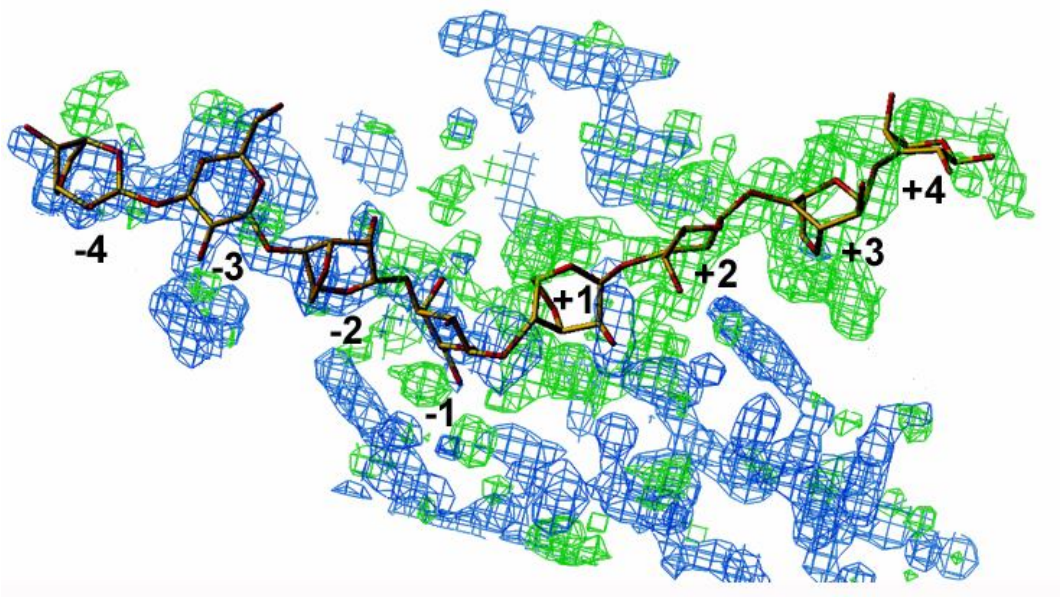


Figure S5. NCS averaged electron density map of the 4 molecules in the a.u. (blue simple Fourier-map of atoms already modelled; green difference Fourier-map), contoured at 2.5 σ, indicative of the presence of disordered agarose units beyond the cleavage site between -1 and +1.

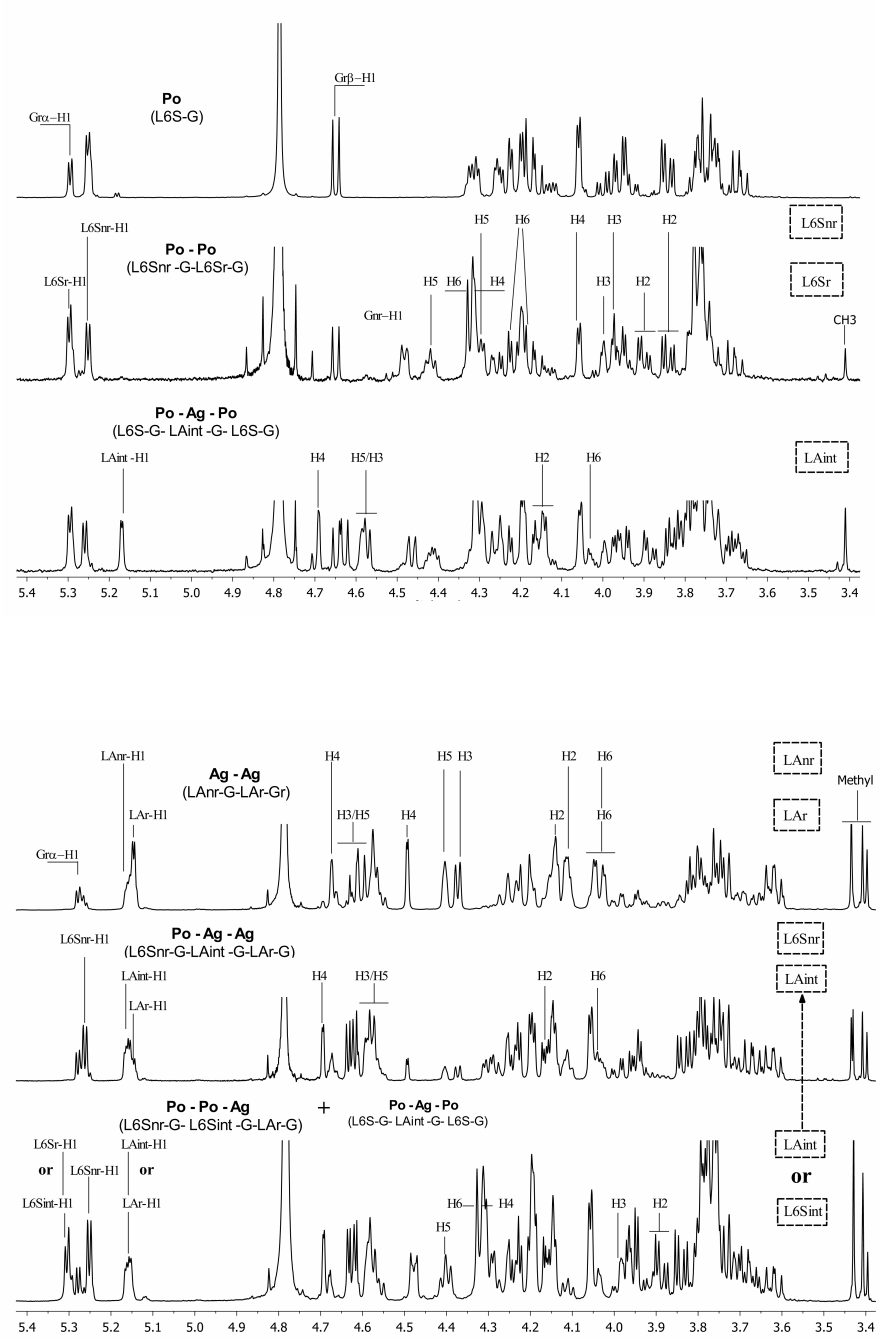


Figure S6. $^{1}$H NMR spectra of purified hybrid oligosaccharides (L6S-G / LA-G) from the degradation products of PorA (a) and AgaB (b) **a**). Tetra (Po-Po) and hexa H1 appeared both unmethylated or methylated (3.4ppm). Partial assignments are indicated above the peaks. **b**). Oligosaccharides producted by AgaB (Tetra-agarose, hexa H2 and hexa H3) are all methylated, and methyl groups could be at three different positions. The H3 hexasaccharide is a mixture of two oligosaccharide, as indicated. Partial assignments that allow identification are indicated above the peaks